



Fig. S1. Character of outcrops at the watershed between the Kopto and Bai-Syut rivers (samples OK-421, OK-422, OK-423, OK-424, OK-425).



Fig. S2. Character of outcrops in the area of Shambalyg village (samples ШБ-1, ШБ-8, ШБ-10).



Fig. S3. Bedrock exposure of tuff conglomerates of the Ondum Formation (site OB22-3), the left basement river terrace of the Wadi-Bala stream



Fig. S4. Bedrock exposure of tuff gravelites of the Ondum Formation (sample OB24-1), the left basement river terrace of the Wadi-Bala stream

In the vicinity of sites OB22-3 and OB24-1, volcanogenic-sedimentary deposits with clast sizes ranging from 15 cm to 5 mm form two crudely bedded packages, 20 m and 50 m thick, respectively, which are interlayered with plagioryholite lava and lavobreccias flows.



Fig. S5. Outcrop photograph showing xenoliths of gabbroids in the granitoids of the DTP-1 association. Site ОБ-54-12.

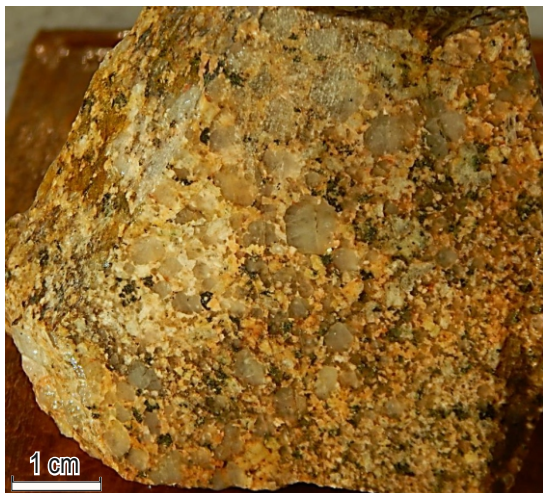


Fig. S6. Sample ОБ-51-12 (plagiogranite).  
Composition: quartz 30%, plagioclase 50%,  
potassium feldspar 5%,  
hornblende (green, replaced by epidote) 1–2%,  
zircon – single grains, ore mineral – 0.n%,  
secondary minerals (epidote, chlorite) 1–2%.

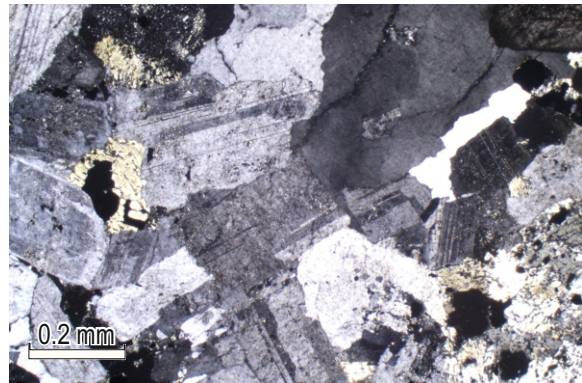


Fig. S7. Microphotograph of thin section  
46026-1 (plagiogranite),  
crossed nicols.  
Composition:  
plagioclase 55%,  
actinolite 20%,  
quartz 10%,  
cordierite 8%,  
albite 2%, chlorite 3%,  
opaque minerals 2%.

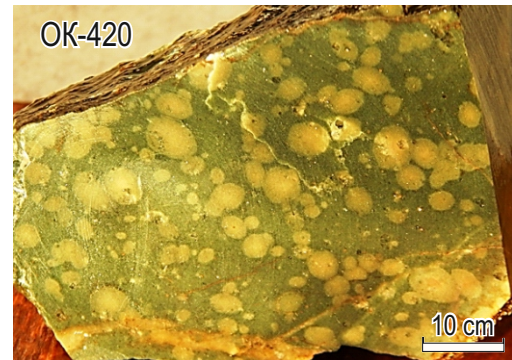


Fig. S8. Samples of felsic volcanics of the Ondum Formation: OK-415 – plagioclase porphyry; OK-420 – rhyolite porphyry.

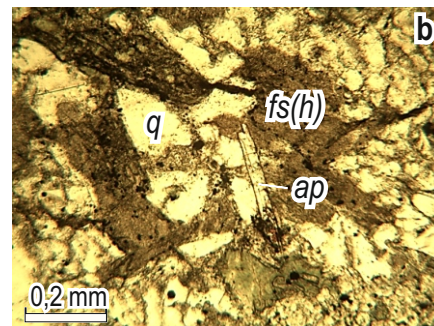


Fig. S9. Macro- (a) and microphotograph (b, parallel nicols) of sample OB22-2a quartz porphyry of the Ondum Complex.

Texture: porphyritic with a microgranular (hypidiomorphic-granular) groundmass (0.02–0.1 mm). Among the phenocrysts, porphyritic quartz grains or clusters of 3–4 quartz grains predominate. Xenogenic rock fragments with a micropegmatitic texture, 1.5–2.5 mm in size, consisting of intergrown crystals of quartz (*q*) and feldspar decomposed to hydromica (*fs(h)*), are present. Apatite (*ap*) crystals occur in the micropegmatite.

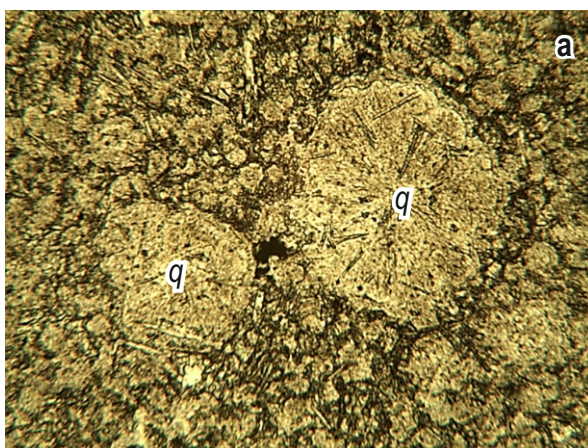


Fig. S10. Microphotographs of plagioclase porphyry from a pebble of tuff conglomerate of the Ondum Formation, sample OB22-36, under parallel nicols (a) and crossed nicols (b).

The groundmass is felsitic, and contains spherulites 0.1–0.3 mm in diameter, consisting of radiating aggregates of quartz (*q*) and albite.

Fig. S11. Microphotographs of zircon from sample OB24-1 tuff gravelite in CL mode (left) and BSE mode (right).  
(0.25–0.1) Grains 01–09, p. 1 of 3.

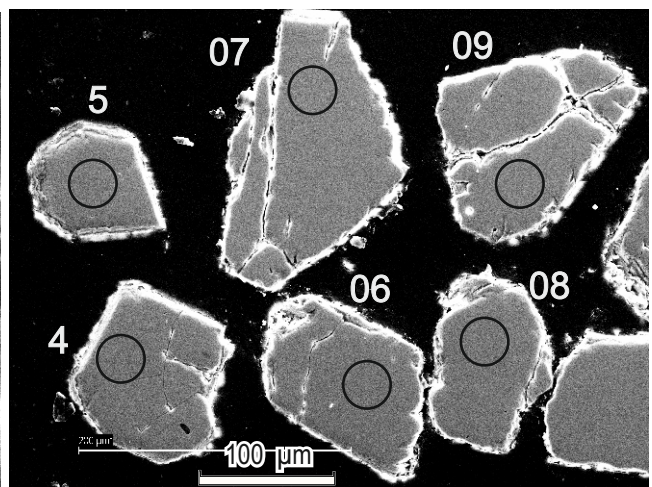
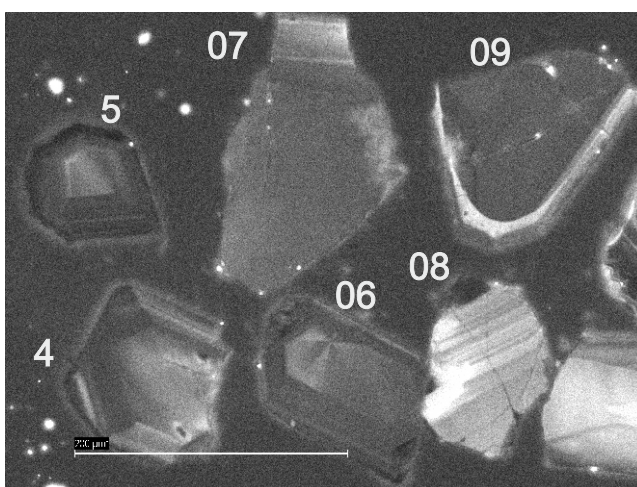
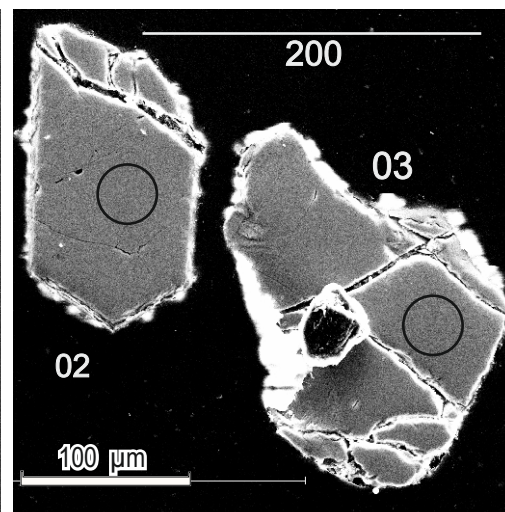
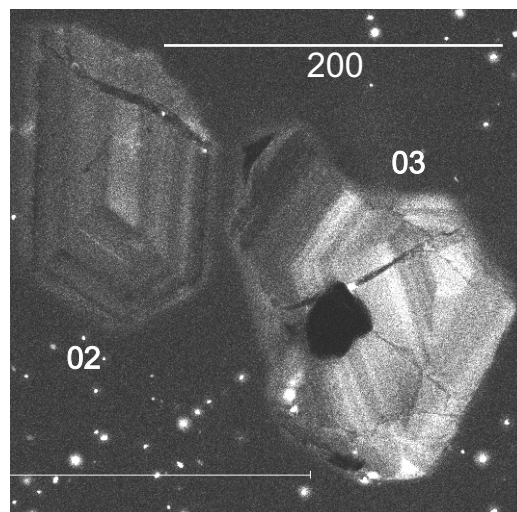
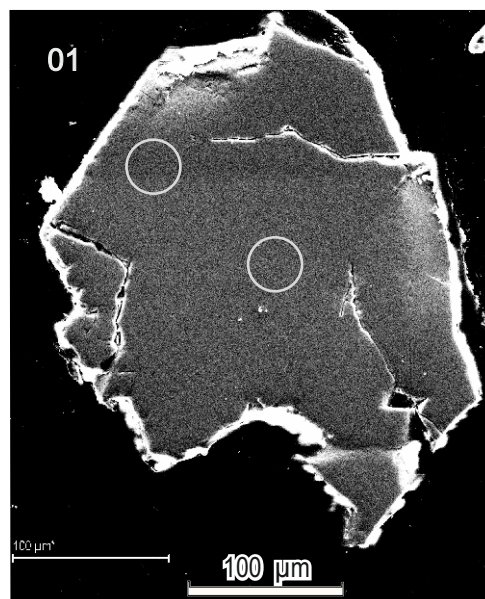
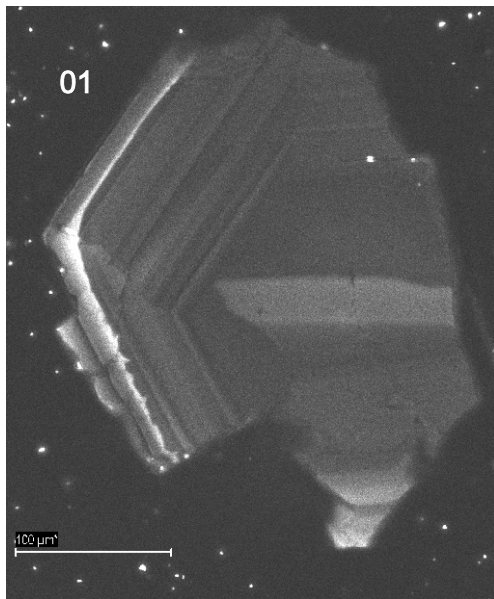


Fig. S12. Microphotographs of zircon from sample OB24-1 tuff gravelite in CL mode (left) and BSE mode (right).  
(0.25–0.1) Grains 10–16, p. 2 of 3.

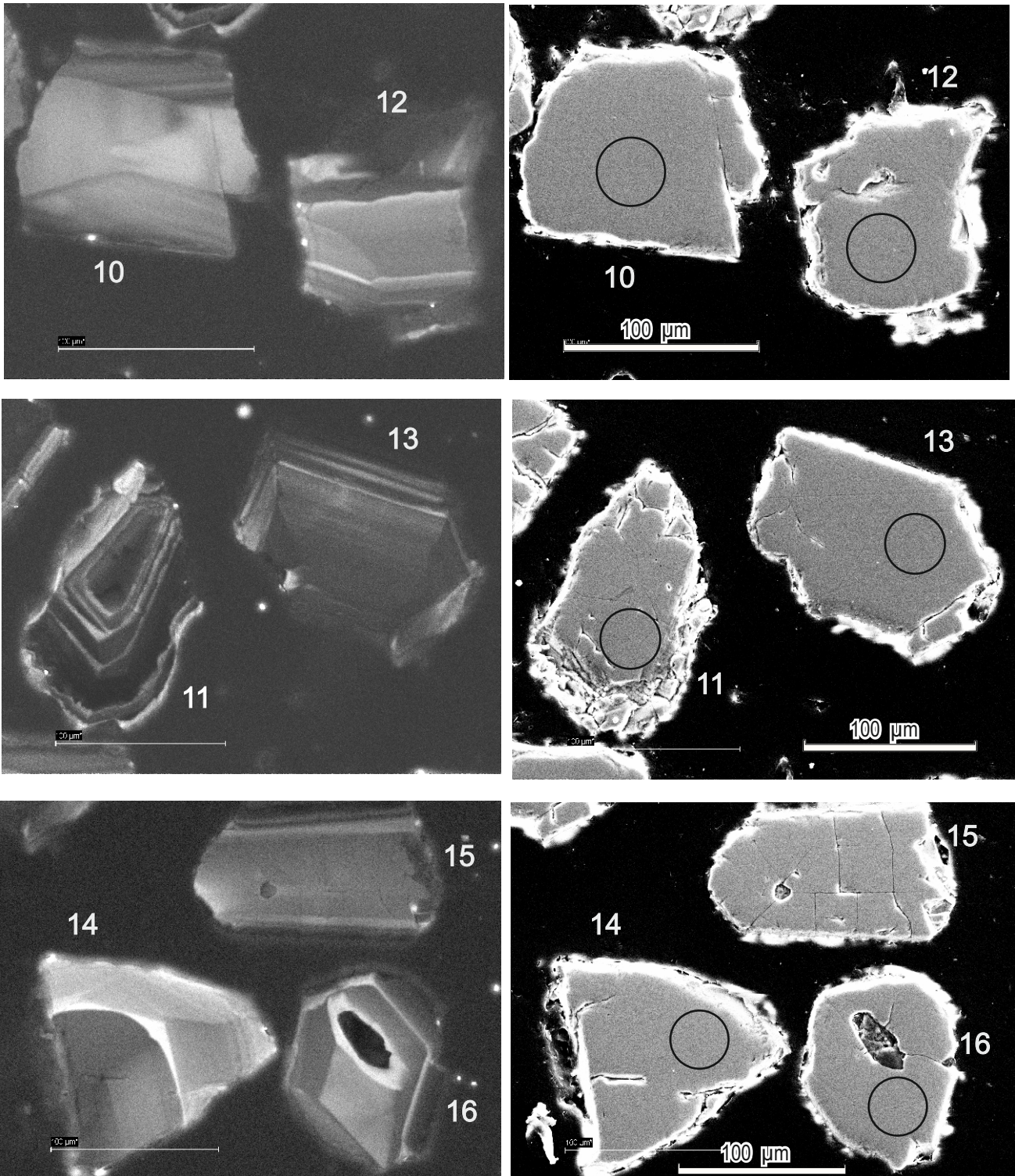


Fig. S13. Microphotographs of zircon from sample OB24-1 tuff gravelite in CL mode (left) and BSE mode (right).  
(0.25–0.1) Grains 17–19, p. 3 of 3.

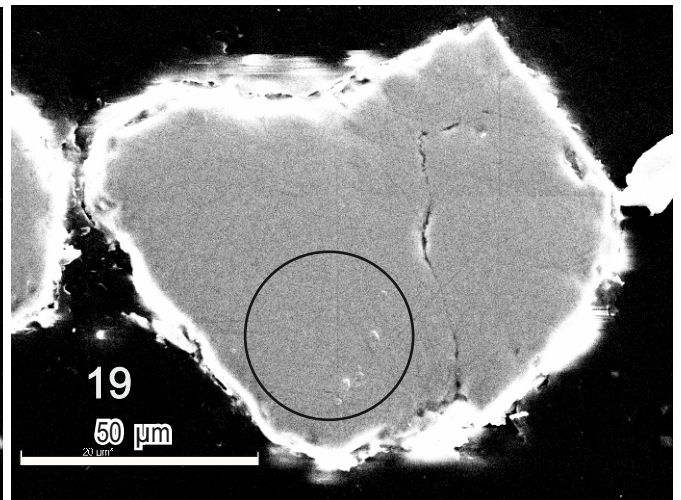
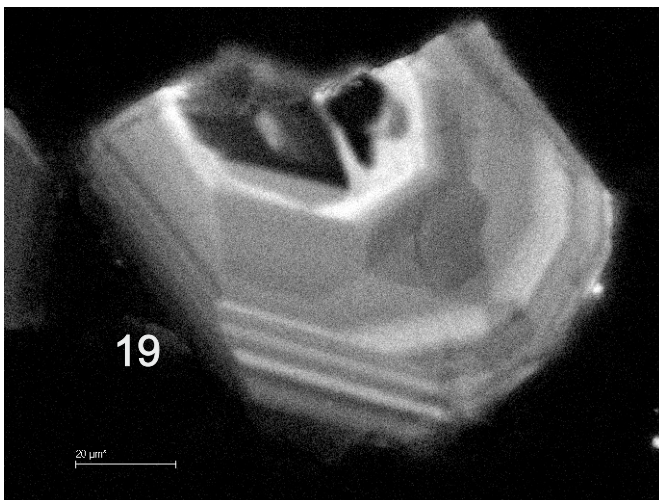
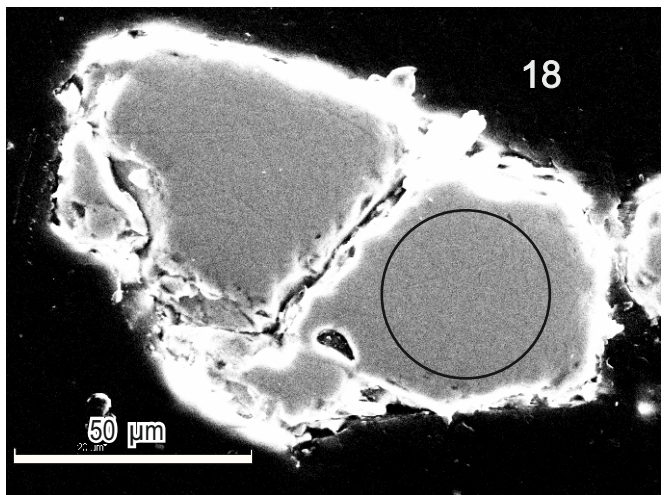
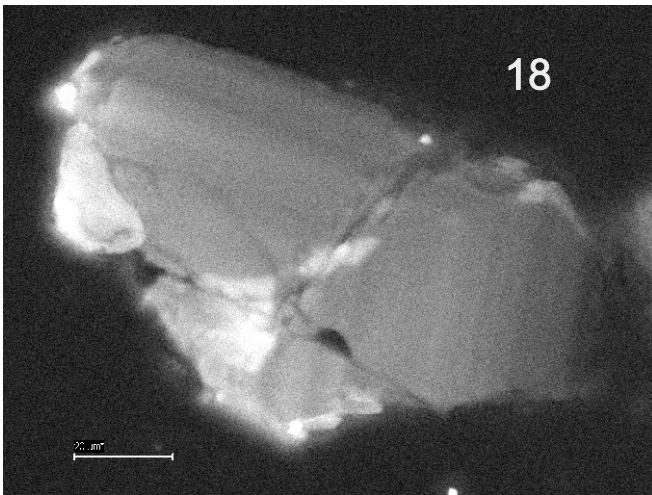
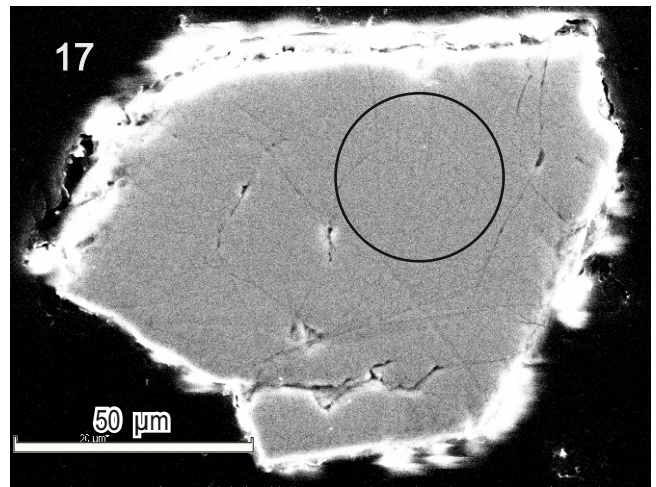
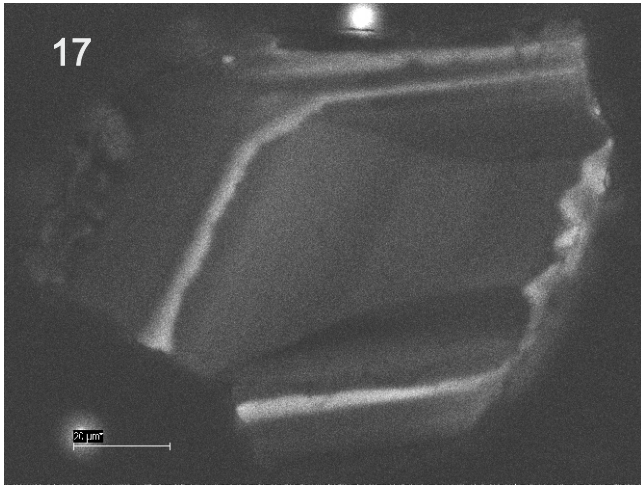


Fig. S14. Microphotographs of zircon from sample O5-51-12 plagiogranite in BSE mode (left) and CL mode (right). (0.25–0.1) Grains 01–35, p. 1 of 5.

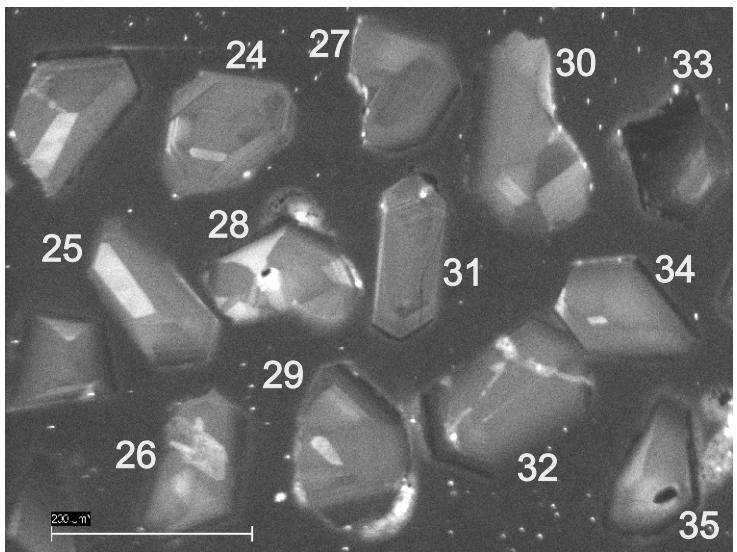
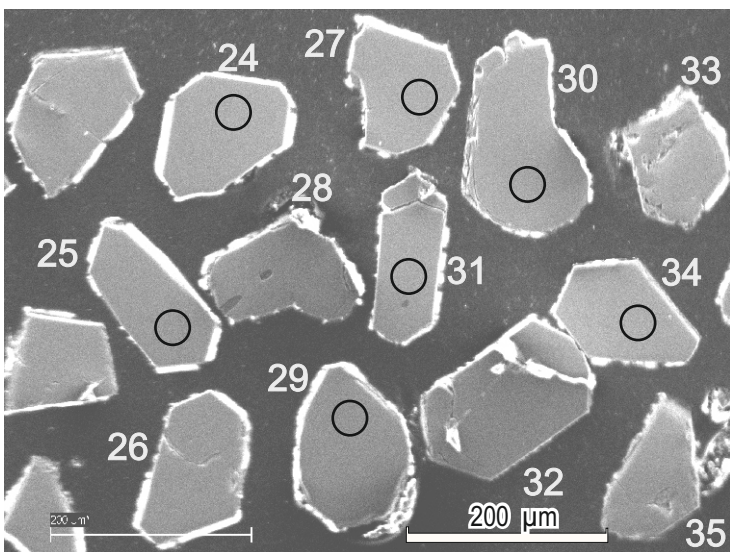
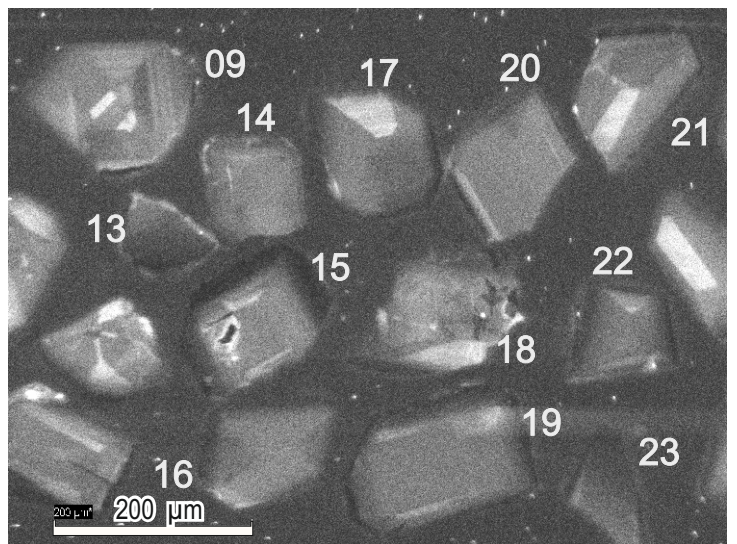
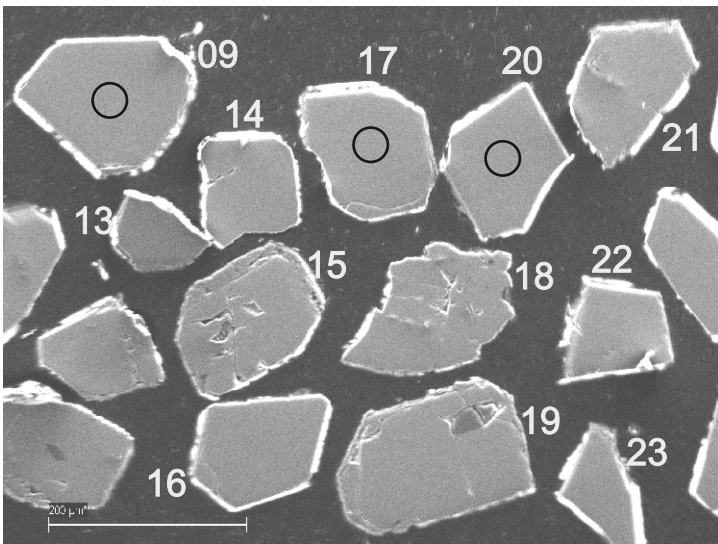
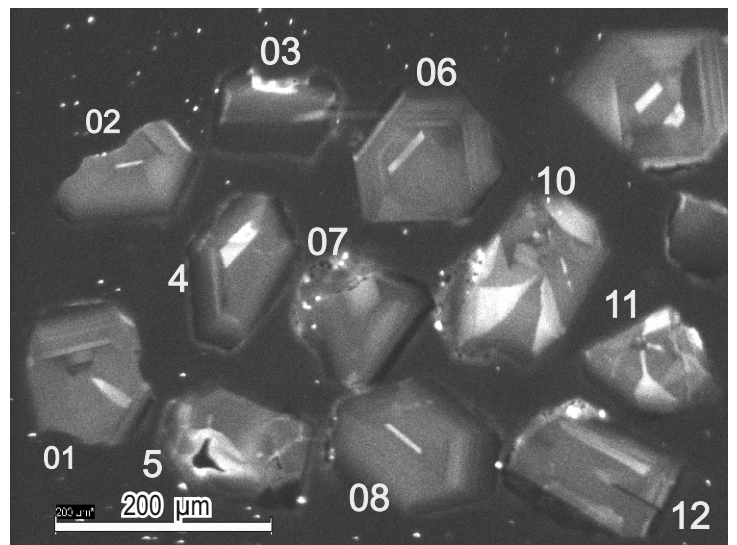
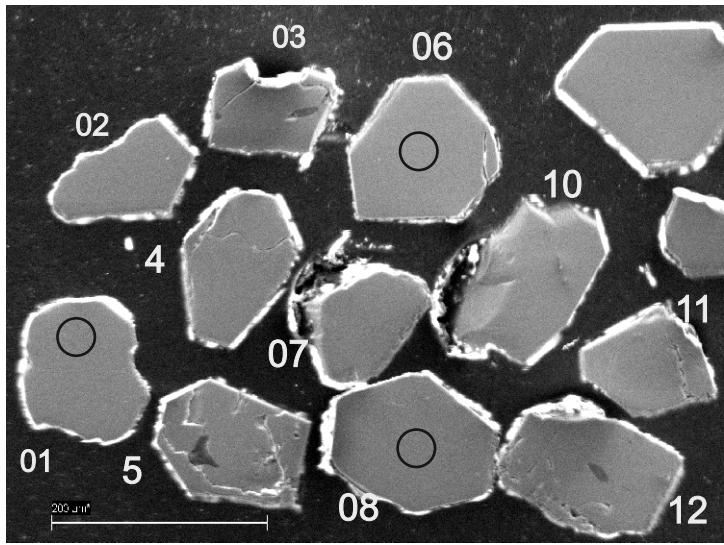


Fig. S15. Microphotographs of zircon from sample O5-51-12 plagiogranite in BSE mode (left) and CL mode (right). (0.25–0.1) Grains 36–71, p. 2 of 5.

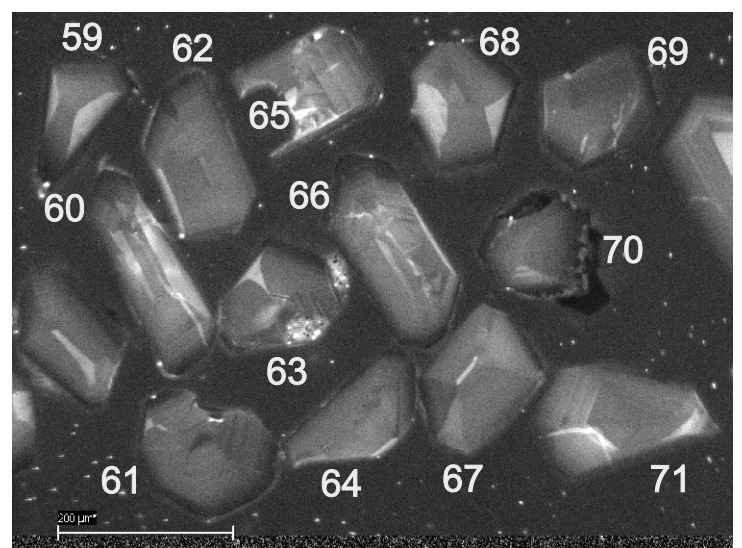
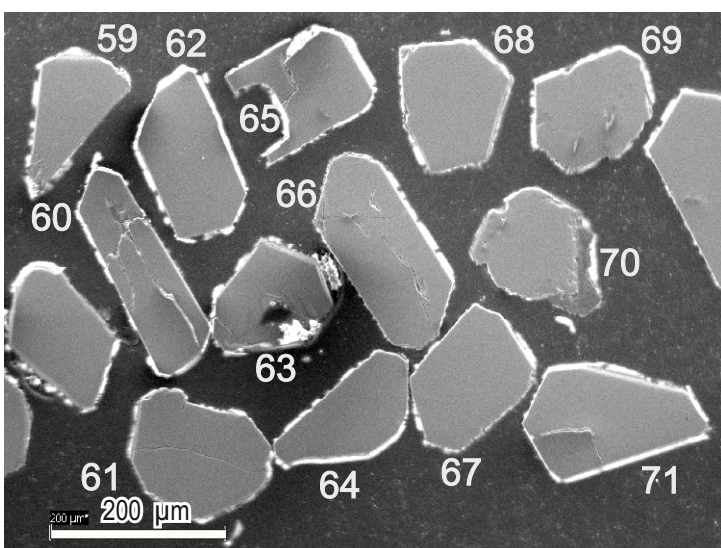
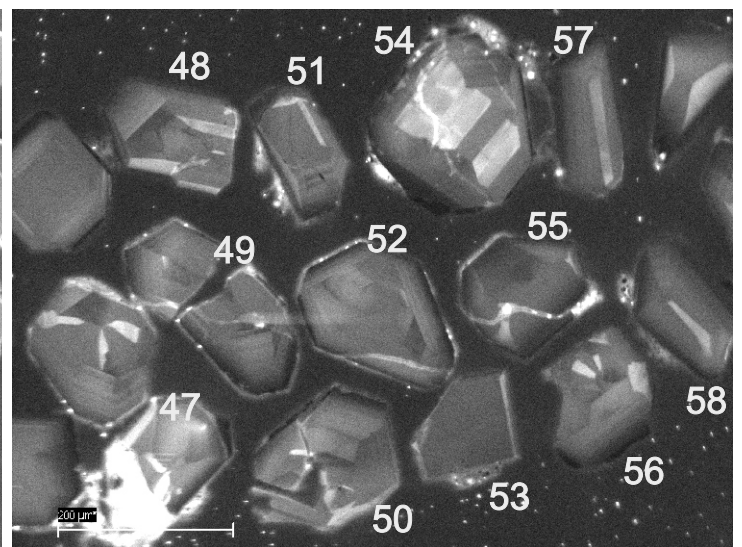
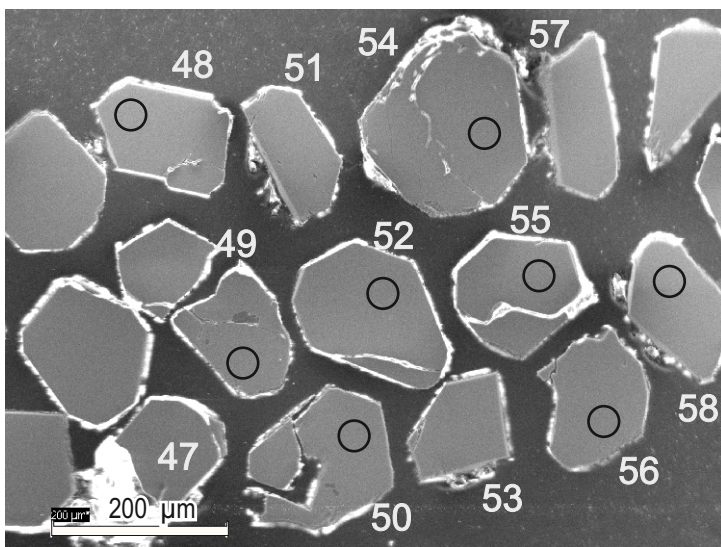
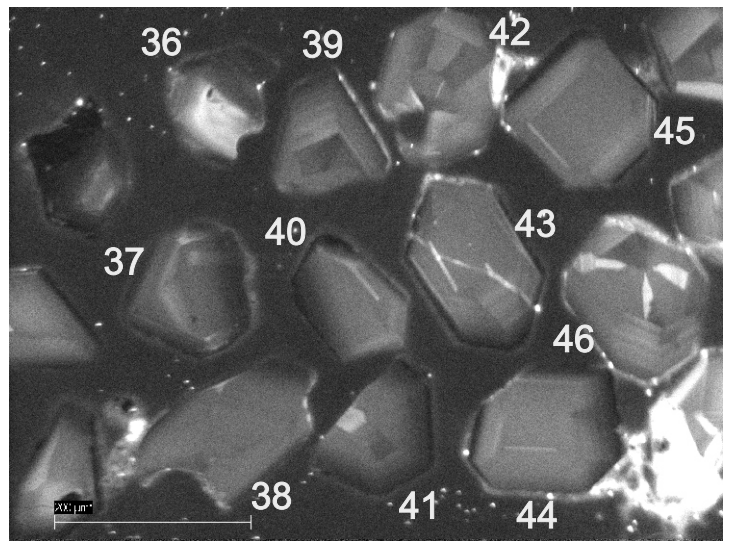
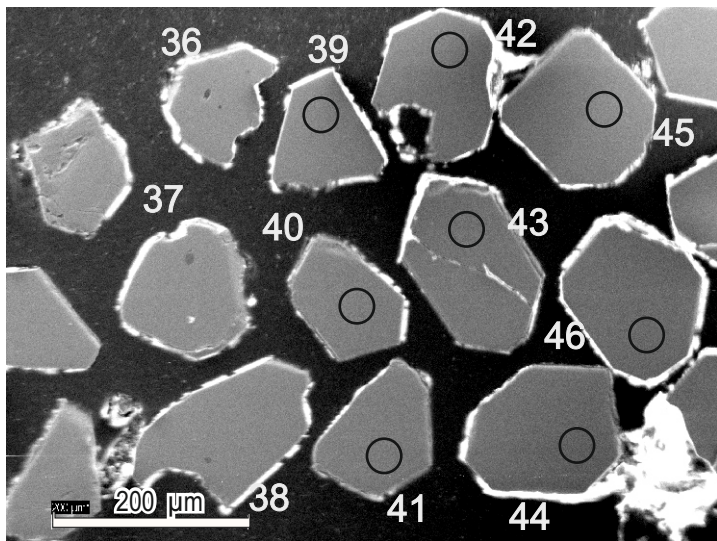


Fig. S16. Microphotographs of zircon from sample O5-51-12 plagiogranite in BSE mode (left) and CL mode (right). (0.25–0.1) Grains 72–102, p. 3 of 5.

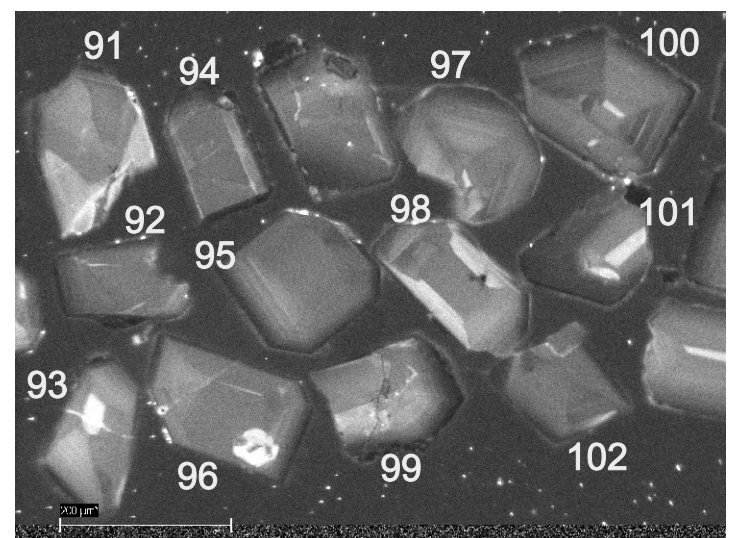
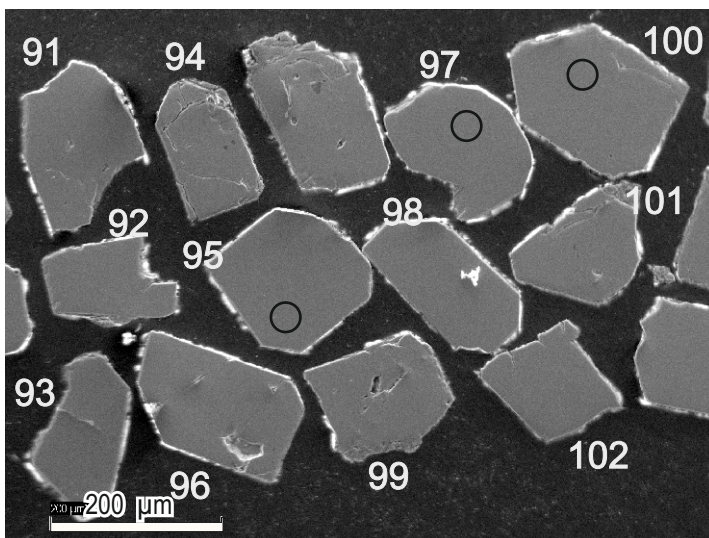
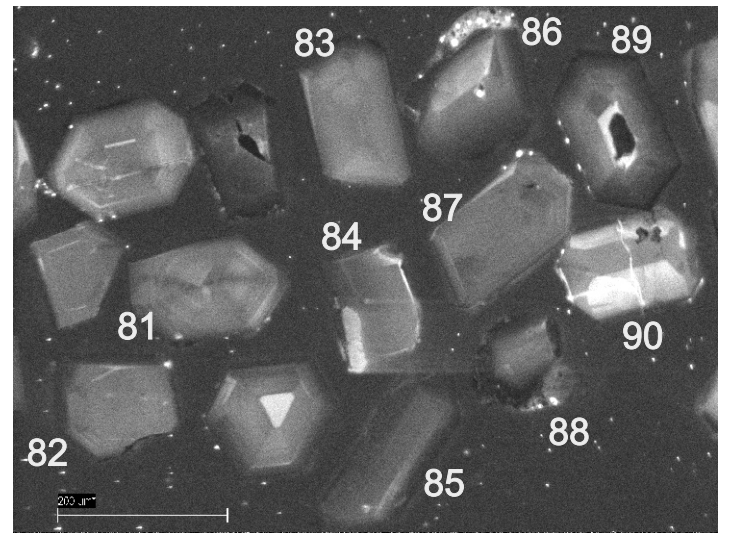
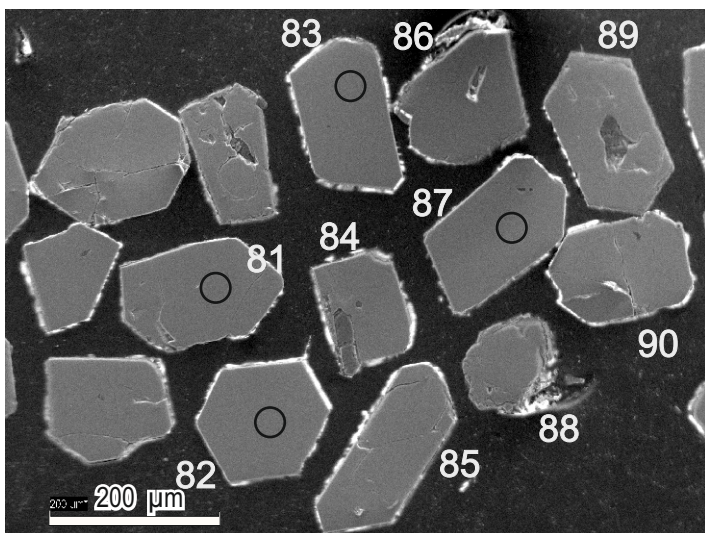
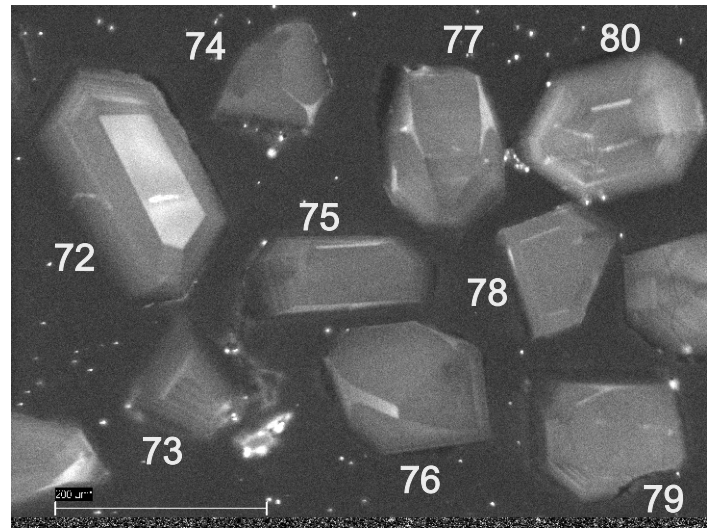
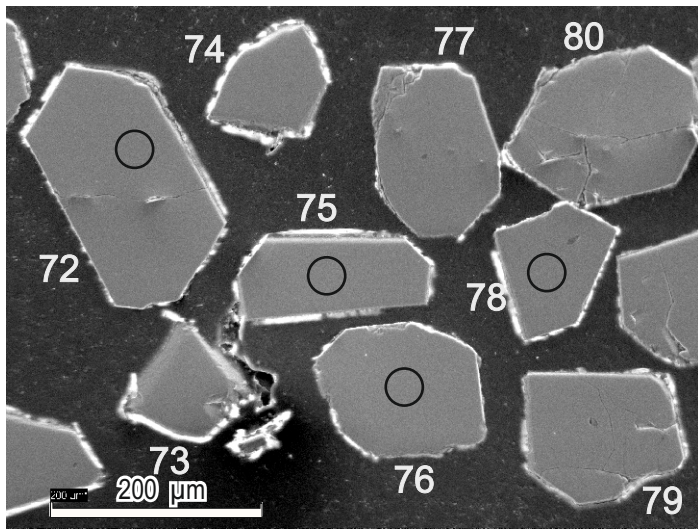


Fig. S17. Microphotographs of zircon from sample O5-51-12 plagiogranite in BSE mode (left) and CL mode (right).  
(0.25–0.1) Grains 103–135, p. 4 of 5.

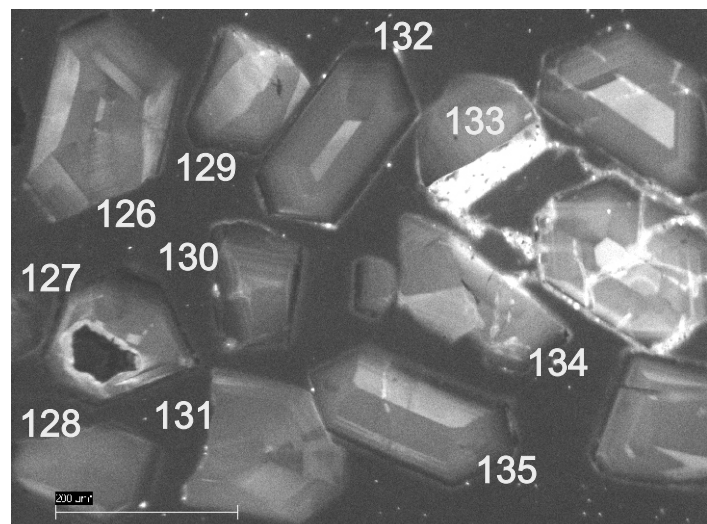
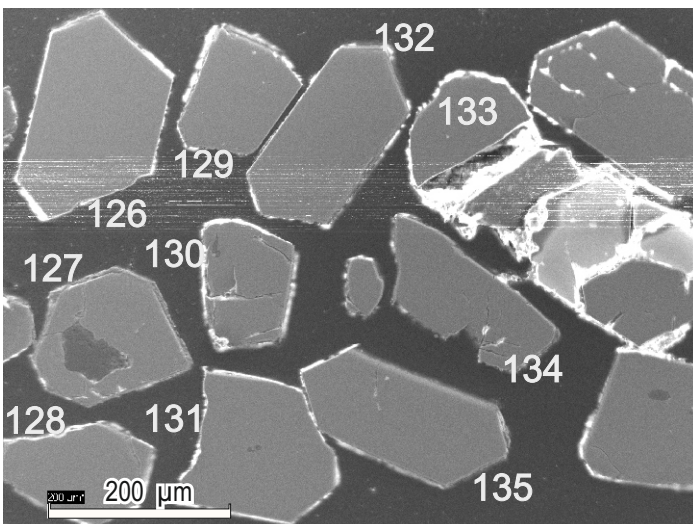
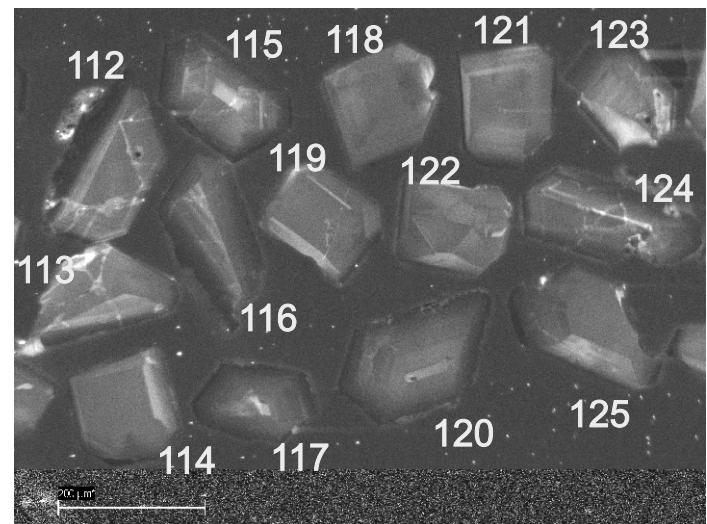
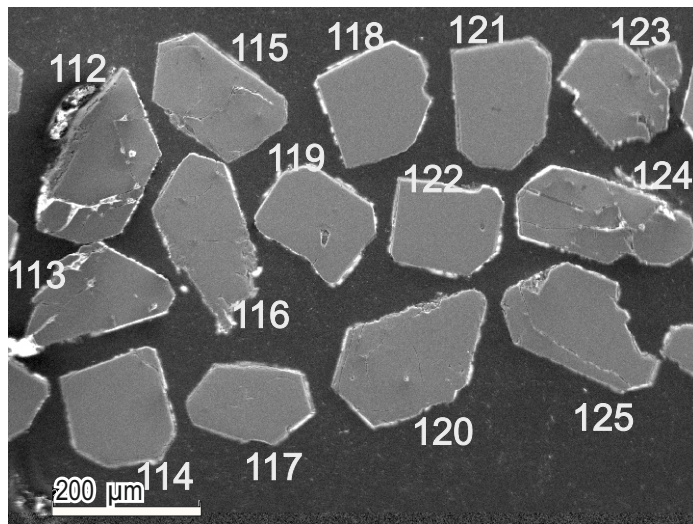
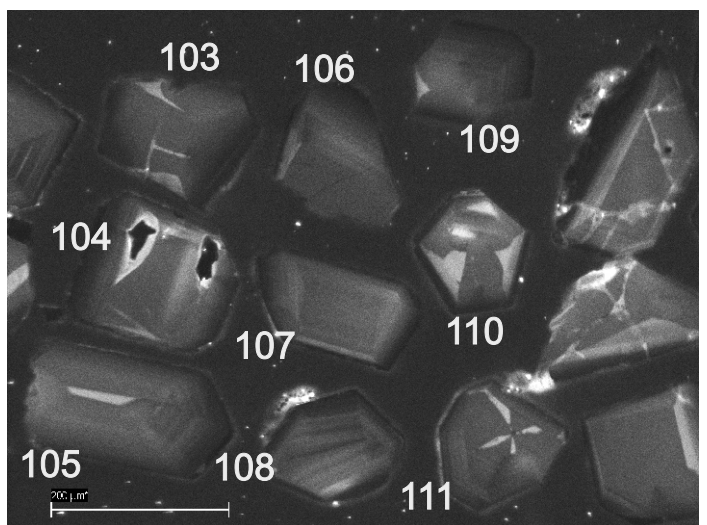
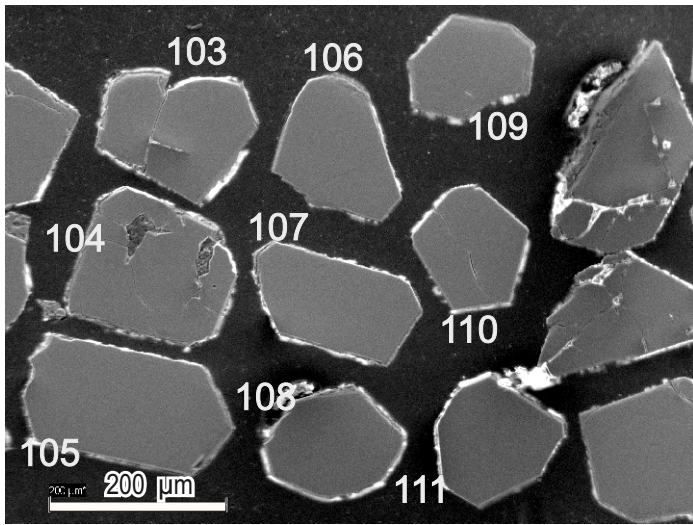


Fig. S18. Microphotographs of zircon from sample O5-51-12 plagiogranite in BSE mode (left) and CL mode (right). (0.25–0.1) Grains 136–148, p. 5 of 5.

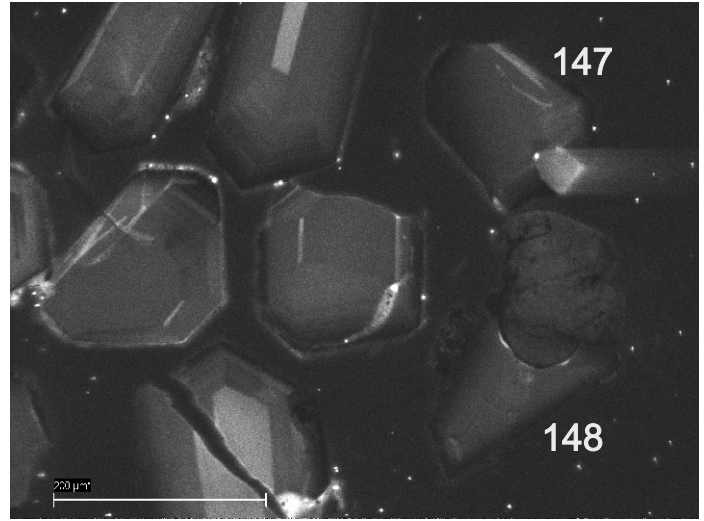
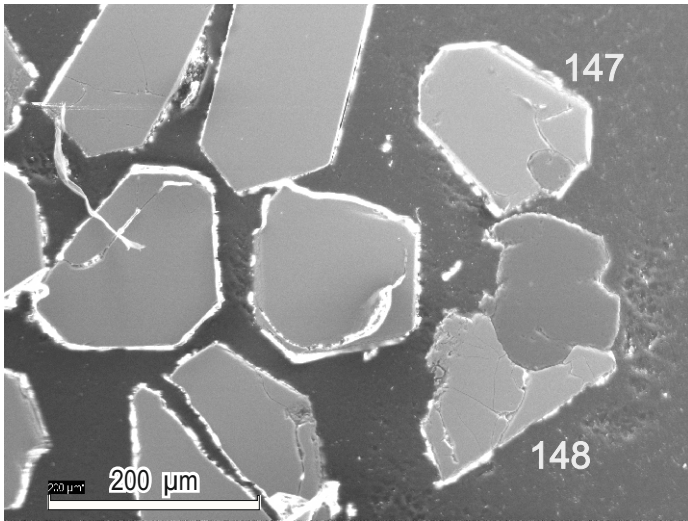
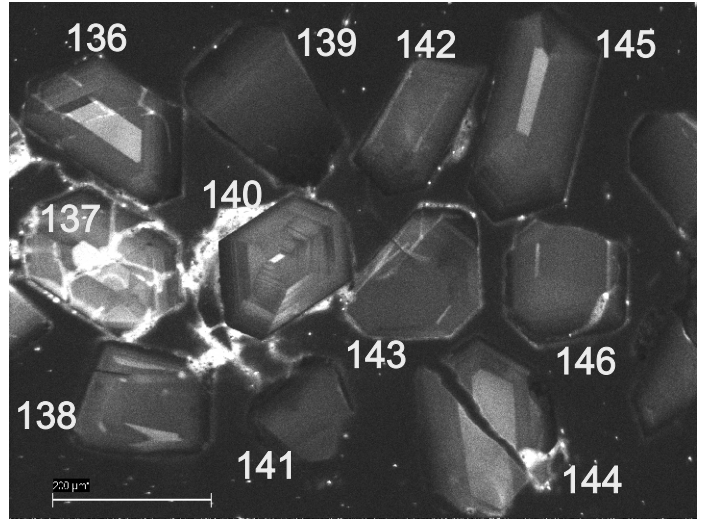
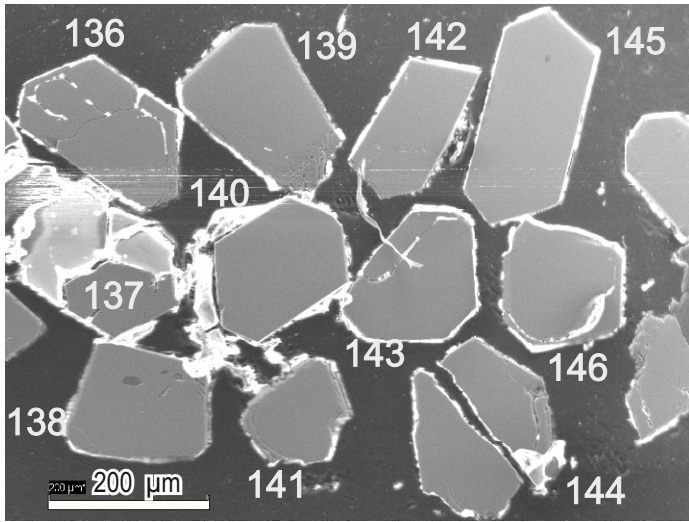


Fig. S19. Microphotographs of zircon from sample 46026-1 plagiogranite in CL mode, p. 1 of 3.

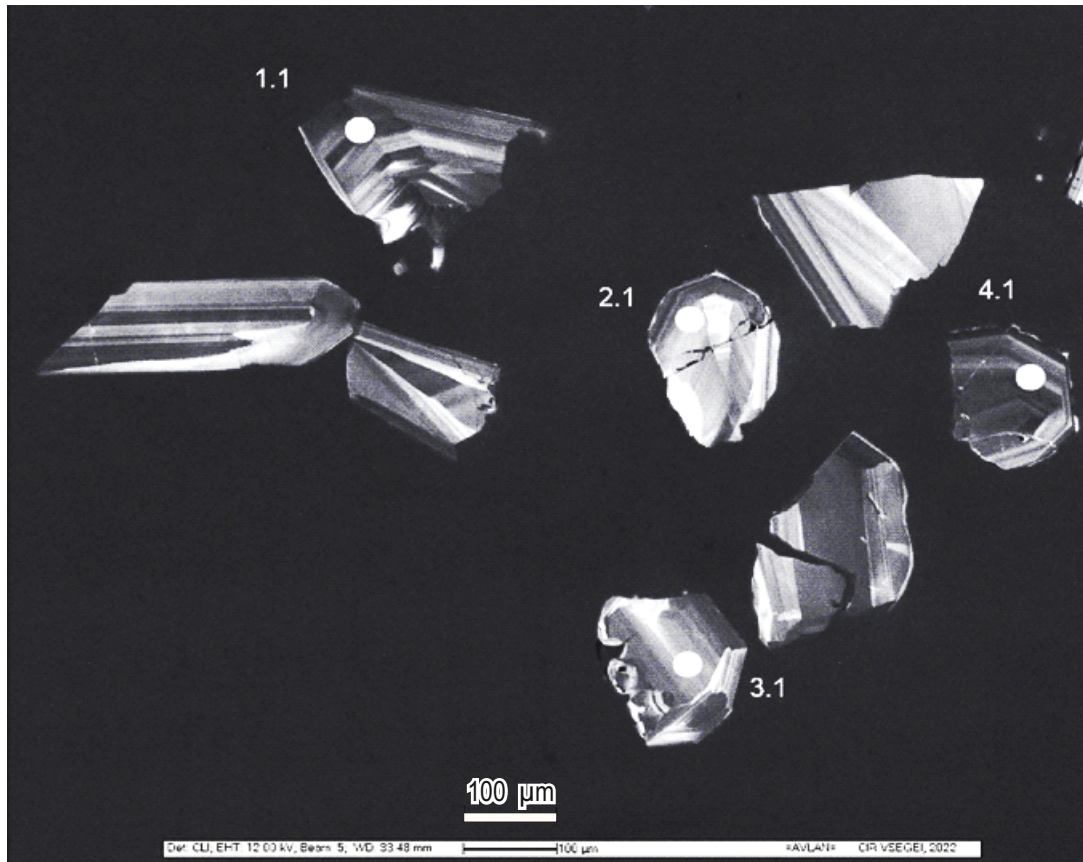


Fig. S20. Microphotographs of zircon from sample 46026-1 plagiogranite in CL mode, p. 2 of 3.

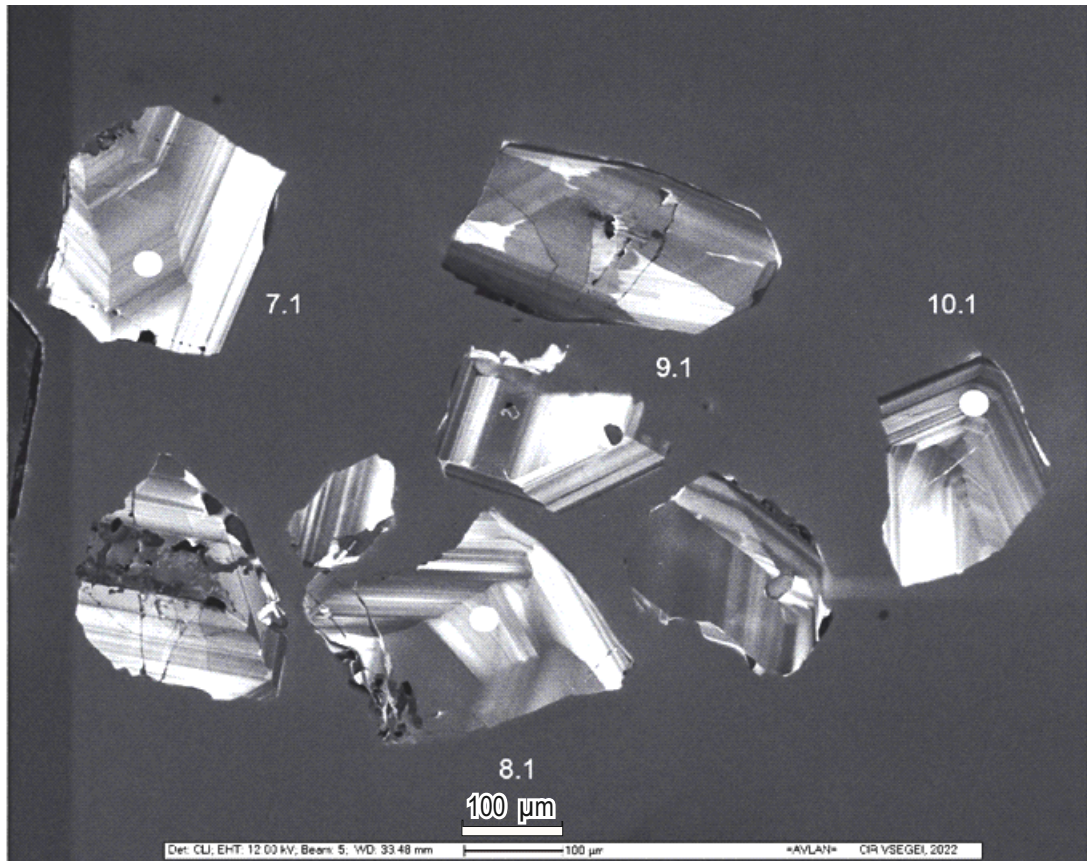


Fig. S21. Microphotographs of zircon from sample 46026-1 plagiogranite in CL mode, p. 3 of 3.

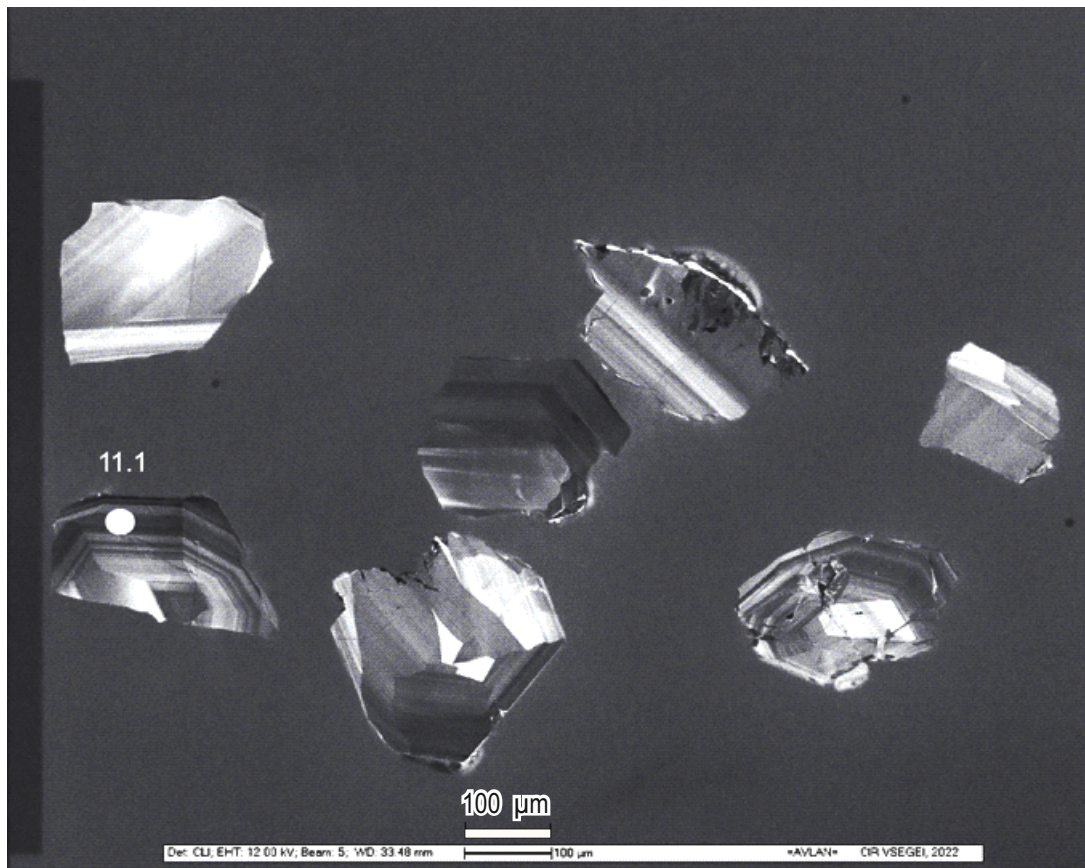


Fig. S22. Microphotographs of zircon from sample 340105 adakite (tonalite) in CL mode, p. 1 of 2.

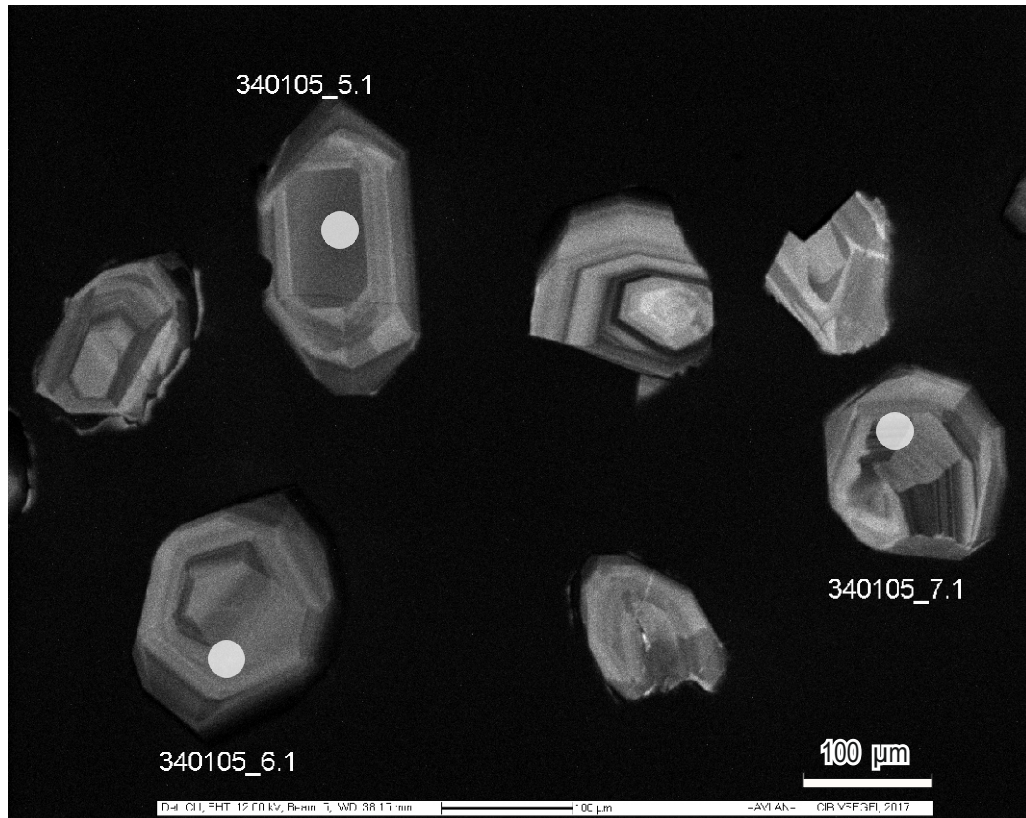
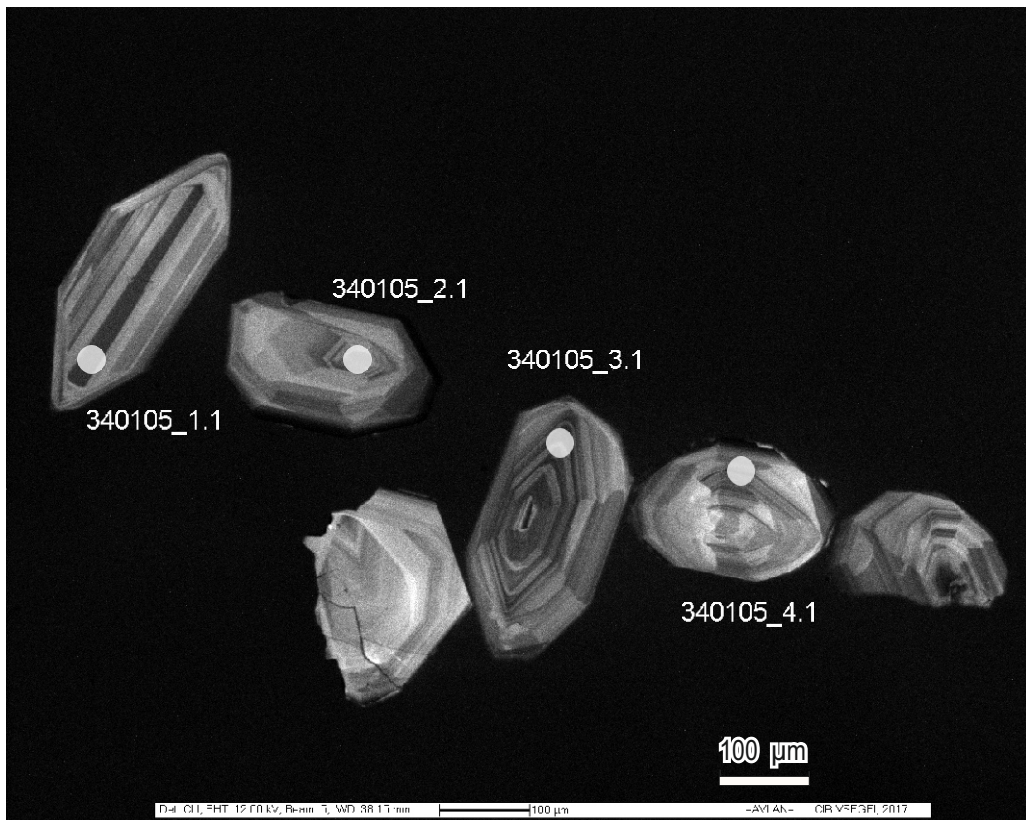


Fig. S23. Microphotographs of zircon from sample 340105 adakite (tonalite) in CL mode, p. 2 of 2.

